

Growth Attenuation with Developmental Schedule Progression in Embryos and Early Larvae of *Sterechinus neumayeri* Raised under Elevated CO₂

Pauline C. Yu^{1*}, Mary A. Sewell², Paul G. Matson¹, Emily B. Rivest¹, Lydia Kapsenberg¹, Gretchen E. Hofmann¹

1 Department of Ecology Evolution and Marine Biology, University of California Santa Barbara, Santa Barbara, California, United States of America, **2** School of Biological Sciences, University of Auckland, Auckland, New Zealand

Abstract

The Southern Ocean, a region that will be an ocean acidification hotspot in the near future, is home to a uniquely adapted fauna that includes a diversity of lightly-calcified invertebrates. We exposed the larvae of the echinoid *Sterechinus neumayeri* to environmental levels of CO₂ in McMurdo Sound (control: 410 μatm, Ω = 1.35) and mildly elevated pCO₂ levels, both near the level of the aragonite saturation horizon (510 μatm pCO₂, Ω = 1.12), and to under-saturating conditions (730 μatm, Ω = 0.82). Early embryological development was normal under these conditions with the exception of the hatching process, which was slightly delayed. Appearance of the initial calcium carbonate (CaCO₃) spicule nuclei among the primary mesenchyme cells of the gastrulae was synchronous between control and elevated pCO₂ treatments. However, by prism (7 days after the initial appearance of the spicule nucleus), elongating arm rod spicules were already significantly shorter in the highest CO₂ treatment. Unfed larvae in the 730 μatm pCO₂ treatment remained significantly smaller than unfed control larvae at days 15–30, and larvae in the 510 μatm treatment were significantly smaller at day 20. At day 30, the arm lengths were more differentiated between 730 μatm and control CO₂ treatments than were body lengths as components of total length. Arm length is the most plastic morphological aspect of the echinopluteus, and appears to exhibit the greatest response to high pCO₂/low pH/low carbonate, even in the absence of food. Thus, while the effects of elevated pCO₂ representative of near future climate scenarios are proportionally minor on these early developmental stages, the longer term effects on these long-lived invertebrates is still unknown.

Citation: Yu PC, Sewell MA, Matson PG, Rivest EB, Kapsenberg L, et al. (2013) Growth Attenuation with Developmental Schedule Progression in Embryos and Early Larvae of *Sterechinus neumayeri* Raised under Elevated CO₂. PLoS ONE 8(1): e52448. doi:10.1371/journal.pone.0052448

Editor: Howard Browman, Institute of Marine Research, Norway

Received: September 5, 2012; **Accepted:** November 13, 2012; **Published:** January 2, 2013

Copyright: © 2013 Yu et al. This is an open-access article distributed under the terms of the Creative Commons Attribution License, which permits unrestricted use, distribution, and reproduction in any medium, provided the original author and source are credited.

Funding: This project was funded by the U.S. Office of Polar Programs, Antarctic Division (NSF grant ANT-0944201 to GEH) (<http://www.nsf.gov>). PCY was supported by a U.S. National Science Foundation (NSF) Polar Programs Postdoctoral Fellowship (NSF-OPP Award 1019340); EBR and LK were supported by NSF Graduate Student Research Fellowships. MS was supported by the Royal Society of New Zealand Marsden Fund (<http://www.royalsociety.org.nz/programmes/funds/marsden/>). The funders had no role in study design, data collection and analysis, decision to publish, or preparation of the manuscript.

Competing Interests: The authors have declared that no competing interests exist.

* E-mail: pauline.yu@lifesci.ucsb.edu

Introduction

The Southern Ocean is predicted to be one of the first major regions to experience the biological consequences of ocean acidification [1,2]. Areas of the global oceans predicted to rapidly become low to undersaturated (Ω < 1) with respect to calcium carbonate (CaCO₃) are considered hotspots of ocean acidification; the waters surrounding Antarctica are particularly close to undersaturation due to both the interaction of seawater with CO₂ at cold temperatures and the transport of remineralized deep water from the conveyor belt [1,3,4]. These changes to ocean chemistry render the calcified biota of the Southern Ocean especially vulnerable compared to warmer, lower latitude coastal areas, because Antarctic organisms already inhabit waters where forming calcium carbonate is more challenging [5,6,7] and are under threat from incursions by decapod predators [8,9,10]. Presently there is emerging data regarding the response of various Antarctic invertebrates to altered seawater carbonate chemistry [11,12,13,14]. To explore the impacts of future acidification due to anthropogenic CO₂ inputs on developmental stability in a key

benthic echinoderm, we utilized the sea urchin *Sterechinus neumayeri* to test the effects of high pCO₂/low pH on early development and larval growth.

We selected an echinoid for our study as echinoderms in general are an important macrofaunal contributor to the carbonate geochemistry of global oceans, and *S. neumayeri* is one of the main contributing species to the standing stock of carbonate in well-sampled regions of Antarctica [15]. They are (along with the asteroid *Odontaster validus*) among the most abundant calcifying benthic species in the shallow benthos and are a dominant grazer species [16]. Because of their relative importance, the effects of climate change, and in particular, ocean acidification, on these organisms is a topic of concern [3,6].

Interestingly, despite the vulnerability of the Antarctic marine ecosystem, we have limited information about present day carbonate chemistry in the Southern Ocean and coastal regions of particular biological importance, such as the Western Antarctic Peninsula. The carbonate chemistry of the Southern Ocean has generally been assessed during oceanographic cruises (e.g. WOCE, JGOFS: [4,17], and others: [18,19]). Recent efforts to enhance

and coordinate oceanographic monitoring in the Southern Ocean have been initiated (Southern Ocean Observing System (SOOS) – www.soos.aq). However, nearshore measurements in the vicinity of shallow benthic macrofaunal assemblages are rare [20]. The availability of new equipment – autonomous pH sensors based on ion-sensitive field-effect transistor (ISFET) pH electrodes – to measure the environmental pH [21] has allowed us to use these data [20] to set the control conditions for our laboratory experiments. These new high frequency time-series measurements indicate that coastal waters near Ross Island (at depths and sites where *S. neumayeri* are present) were pH 8.02–8.04 on average during the austral spring of 2010 [20]. The pH profiles indicate that indeed these subzero waters are somewhat more acidic than warmer open ocean waters of the northeastern Pacific and other global ocean time-series locations (e.g. Hawaii Ocean Time Series), and also that the variability around Ross Island as compared to other coastal regions is low [22]. Under near-future IPCC models of the “business as usual” A1FI scenario (2007), the surface waters of the Southern Ocean will be undersaturated on average in less than 50 years time; we chose to bracket our experimentally elevated pCO₂ levels slightly below and above that estimate to determine physiological responses to those challenges. Additionally, the oceanography of the Southern Ocean is expected to accelerate the undersaturation of shallow waters due to interactions with carbonate-poor deep water during the austral winter [4]; depending on the developmental schedule and spawn timing of *S. neumayeri*, these winter months of low calcium carbonate saturation could coincide with larval settlement [23].

In light of the unique biology of polar organisms and the accelerated pace of changes in these regions, the adaptability of polar organisms to future environmental conditions has become a research focus for the polar biology community, with a particular emphasis on adaptive physiology [22,24,25]. Recent studies examining the effects of ocean acidification on polar invertebrates have found mostly negative effects on calcifying species [11,12,14,26,27,28], but a few studies found no effects on fertilization or early development in Antarctic urchins and non-calcifying species [13,29,30]. The breadth of the study organisms is obviously limited, and several studies were conducted using temperate seawater sources. Studies on adult organisms have also predominated due to availability of baseline physiology data on particular species, while in contrast the developmental physiology of *S. neumayeri* is well-characterized from prior research [31,32,33,34], thus making it an excellent system for ocean acidification studies on early life history stages.

A growing body of literature suggests that early life history stages may be vulnerable to ocean acidification [35,36] (see review in [37]). Given the low carbonate saturation conditions, and the long pelagic larval duration of planktotrophic Antarctic echinoderms [23], investigation of the tolerance of these species to elevated pCO₂ includes an extended temporal dimension not possible with some temperate or tropical species: development to pluteus in *S. neumayeri* occurs in ~17 days at –0.3°C compared to 5 days to pluteus at 17°C in the temperate confamilial species *Echinus esculentus* [38]. Thus, considering the variation of physiological responses to ocean acidification that has been observed between species of echinoids [37,39], *S. neumayeri* provides an important study model for this environment. The slow developmental rates of *S. neumayeri* provide ample opportunity to look for morphological signs of developmental delay, especially during critical developmental events such as gastrulation, and early skeleton deposition. For this study we employed a culturing apparatus (described in [40]), which allows us to raise embryos through advanced 4-arm pluteus at different pCO_{2S} in continuous

flow-through cultures. Our results provide a mixed picture for this Antarctic species where no early developmental delay at benchmark morphological development points was observed under elevated pCO₂, but significant morphometric differences between treatments were observed later in development. Allometric variation was altered under elevated pCO₂, suggesting that growth differences may contribute to observed size differences. The negative growth response of these larvae to pCO₂ levels of near-future climate scenarios suggests that negative impacts on calcifying species will manifest sooner in hotspots of ocean acidification such as the Antarctic.

Methods

Animal Collection and Culturing

Adult *Sterechinus neumayeri* were collected by SCUBA from a benthic site in McMurdo Sound near Cape Evans, Ross Island, Antarctica (S 77 degrees 38.059' E 166 degrees 24.905'). No permits or permissions were required for the collection of animals at this location and the study site is not privately owned. *S. neumayeri* is not an endangered or protected species, and adult animals were returned to the collection site at the end of the experiment. Adult urchins were maintained in seawater tables in the aquarium at the A. P. Crary Science and Engineering Center (hereafter referred to as “Crary Lab”) at McMurdo Station, Antarctica, at –1.5 to –1.0°C (ambient incoming seawater temperature) until spawning. Spawning was induced by intracoelomic injection of ice-cold 0.5M KCl. Eggs from 20 females were collected into 0.35 μm-filtered seawater and kept on ice, while sperm was collected “dry” from a single male and kept on ice until use. Eggs were combined, and fertilized together as a single batch and enumerated. Embryos were checked for fertilization success (>95%) and distributed equally into 15 buckets (5 replicate buckets for each pCO₂ treatment level, see next section) at 10 embryos ml⁻¹ within 1 hr of fertilization.

Embryos and larvae were cultured in the CO₂ culturing system described in Fanguet *et al.* [40] for 30 days. At intervals, larvae were sampled by reverse siphoning and combined between replicate buckets for analysis. Samples were fixed in 4% formaldehyde, saturating NaBO₃-buffered seawater (pH=9.0) and stored at 4°C for developmental stage scoring. Samples for microscopy and morphometrics were kept live on ice until ready for imaging the same day of collection; this was routinely conducted within 18 hours of sampling.

While larvae of *S. neumayeri* are competent to feed at the “prism” stage (roughly 2 weeks post-fertilization in our cultures) we chose not to feed the larvae in this experiment, for both logistical and experimental reasons. First and foremost, we do not have single-species cultures of Ross Sea phytoplankton optimized for feeding echinoderm larvae. Secondly, previous studies with fed larvae of *S. neumayeri* utilized non-native temperate phytoplankton [23,34]; this approach is unfeasible with the flow-through system [40] as it presents an unacceptable biosecurity risk. While we recognize that maintaining pluteus larvae unfed for 2 weeks might impose an additional physiological stressor, Marsh *et al.* [34] demonstrated that total larval lengths ([34] Fig. 3A: “body”) of unfed larvae (57d) were not statistically different from larvae cultured with “natural” seawater (filtered to 80 μm, but without algal amendment) during the late austral spring in McMurdo Sound, when there are low food conditions [41]. Further, arm lengths of fed and unfed larvae were not statistically different until 40 days of age [34]; this invariance is within the time frame of the current experiments, and therefore the absence of food would not necessarily affect our results.

CO₂ Culturing System

Three treatment pCO₂ levels (410-control, 510 and 730 μatm) and 5 replicates per treatment were established. Modifications to the system [40] included the use of additional insulation on water tubing to maintain temperatures near −1.5°C, and pumping gas at the treatment levels into the headspace of the buckets. Seawater chemistry was monitored via daily pH readings (spectrophotometric pH_{Ts}: [41]) (Shimadzu Instruments, Japan) and Total Alkalinity measurements (open-cell titration: [41]) (Mettler-Toledo). Temperature and pH of all buckets, both reservoirs and larval culture buckets, were monitored. Daily Total Alkalinity samples from treatment reservoirs were poisoned with mercuric chloride (0.02%: [42]) for preservation during storage prior to analysis. Salinity was measured from discrete reservoir samples (3100 Conductivity Meter, YSI). Carbonate chemistry parameters were calculated using CO2Calc [43].

Developmental Stage Scoring

Embryo/larval samples were combined from the five replicate culture buckets for morphological staging to average out any minor temperature effects and to smooth out differences between replicate cultures as samples for morphometrics were also pooled [44]. Samples were staged on a Sedgewick Rafter slide and transects run across the slide until at least 200 embryos/larvae were staged. Development was scored at 10 developmental points during development, at intervals corresponding to major developmental and morphological changes [23,34].

Microscopy and Image Analysis

Larvae were gently fixed with a 10 μl drop of 4% NaBO₃ buffered formaldehyde and immediately wet-mounted on slides for photography. Brightfield and Phase images were captured with a Zeiss Axioskop 50 and a SpotCAM. Brightfield DIC and Polarized light images were captured with a Nikon Petrographic Scope and a Canon PowershotA630. All images were calibrated with a stage reticule with 10 μm resolution and analyzed with ImageJ.

Morphometric measurements of spicules and total lengths are shown in Fig. 1. At days 12 and 15, the nascent anterolateral arm (ALA) rod of late gastrulae and prisms was the axis most easily visualized with the embryos lying on the ventral surface. The ALA rod length was measured from the origin of the triradial center to the tip of the rod (Fig. 1A). At days 20 and 30, only plutei oriented with their oral side facing up were imaged, so as to keep the postoral arms in the same plane of focus as the aboral tip of the larva (Fig. 1B). Postoral arm (POA) rod length and body rod length (Fig. 1C) were measured independently of the total body length on a polarized light duplicate image.

Statistical Analyses

Regressions, ANOVAs and F-tests were performed using MS Excel with the StatPlus:mac plug-in (AnalystSoft Inc.). Due to the high variance in morphometric measurements between individuals, PERMANOVA [45], which is insensitive to non-normality of data, was employed for statistical analyses. Permutational analysis for homogeneity of multivariate dispersion, PERMANOVA and permutational pairwise analyses were performed on untransformed morphometric data using the “vegan” package [46] for R, and the independent PERMANOVA and PERMDISP2 programs [47].

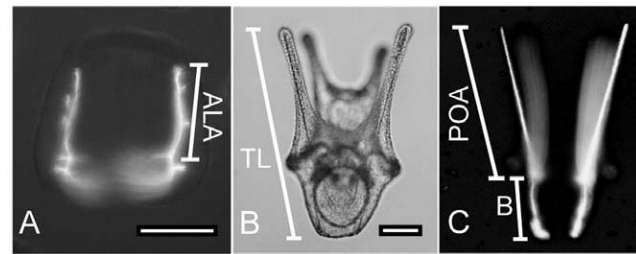


Figure 1. Morphometric measurements of spicule elements and total lengths at prism and pluteus stages. Scale bar shown in lower right corner of A and B = 100 μm. A) A prism stage larva (15 days) visualized under cross-polarized illumination. The ALA rod length (ALA) was measured from the origin of the triradial center to the tip of the spicule rod. B and C) A pluteus larva (30 days) visualized under brightfield (B) and cross-polarized illumination (C). Plutei oriented with their oral side facing up were imaged with the postoral arms in the same plane of focus as the aboral tip of the larva. Total length (TL) was measured from the tip of the postoral arm rod to the aboral tip of the body. Postoral arm rod length (POA) was measured from the tip of the postoral arm rod to the origin of the triradial center, and body rod spicule length (B) was measured from the origin of the triradial center to the aboral tip of the body rod.
doi:10.1371/journal.pone.0052448.g001

Results

Culturing Conditions

Once stable carbonate chemistry conditions were established in larval culture containers, we were able to culture embryos continuously for 30 days, from shortly after fertilization to advanced 4-armed pluteus. Seawater conditions in the Crary Lab aquarium were fairly representative of water conditions in McMurdo Sound. The salinity was almost invariant (Fig. 2A), remaining at 34.8–34.9‰ over the course of the 30-day experiment. The alkalinity values (Fig. 2B) were slightly more variable, but were not significantly different between treatments over the time-course (n = 30, ANOVA, p > 0.1) with the average alkalinities of the three reservoirs running at 2328.5 (±13.0 SD), 2330.5 (±10.5) and 2331.3 (±15.5) for the 410 μatm (control), 510 μatm and 730 μatm pCO₂ treatments respectively. While the environmental seawater temperature was −1.9°C in McMurdo Sound, the incoming seawater in Crary Lab was consistently over a degree warmer, especially given the controlled air temperature within the lab. Water temperatures (Fig. 2C) averaged −0.3 (±0.2), −0.3 (±0.2) and −0.4 (±0.2) °C (n = 5 each treatment, ± SD) for the three treatment levels (410 control, 510 and 730 μatm respectively), with the overall average over time being −0.3°C (±0.2 SD). Averaged pH_{Ts} (Fig. 2D) and pCO₂ (Fig. 2E) (n = 5 each treatment, ± SD) over the time course of the experiment showed acceptable consistency within each treatment despite the variation in alkalinity and temperature over time. Average in-situ pH_{Ts} values over the duration of the experiment were 8.027 (±0.005 SD), 7.937 (±0.005) and 7.793 (±0.007) for the 410 μatm (control), 510 μatm and 730 μatm pCO₂ treatments respectively. Average pCO₂ levels over the duration of the experiment were 408.6 (±6.2 SD), 512.0 (±7.0) and 730.2 (±14.0) μatm for the 3 treatments. Average aragonite saturation values (Ω_{ara}) for the three treatments were 1.35 (±0.02 SD), 1.12 (±0.01), and 0.82 (±0.01).

Developmental Progression

The development of *S.neumayeri* embryos in our culture system followed a developmental schedule slightly accelerated relative to a previously published schedule for cultures grown at McMurdo

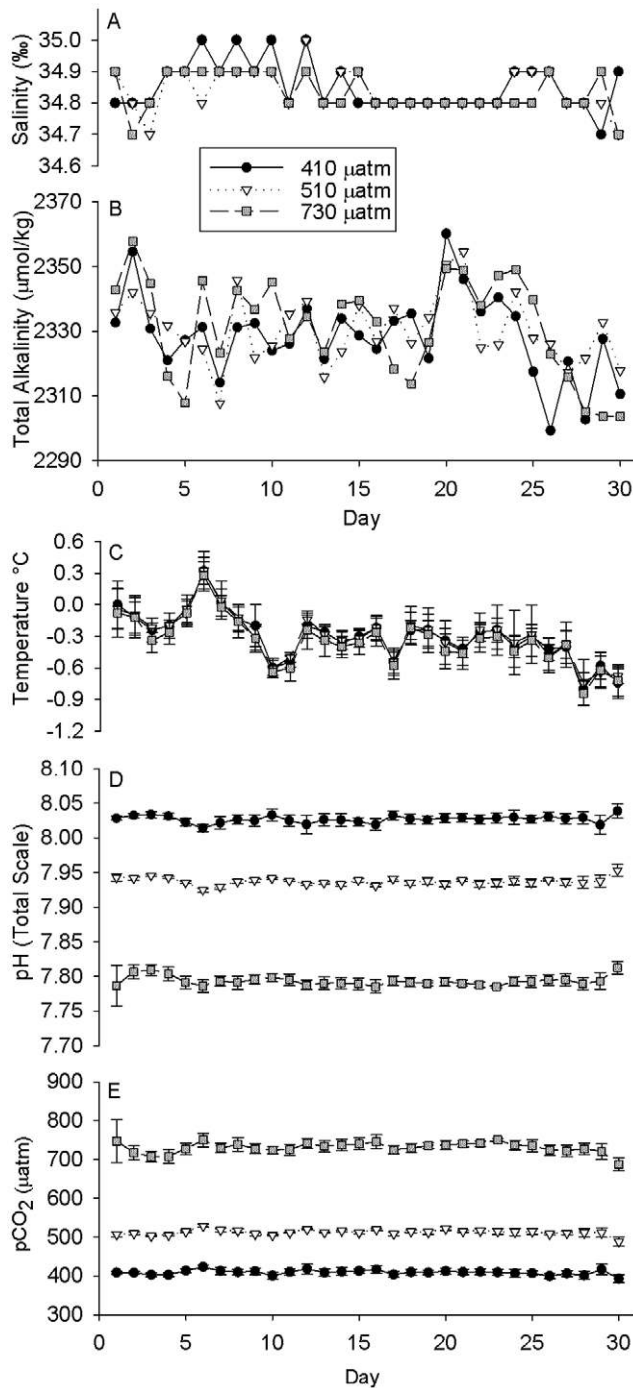


Figure 2. Summary of seawater chemistry. Daily measurements of salinity (A) and Total Alkalinity (B) in the three reservoir buckets for the three treatment levels 410, 510 and 730 μatm . Total Alkalinity was not significantly different between treatments over the duration of the experiment ($n=30$, ANOVA, $p>0.1$). Averaged daily measurements of temperature (C) and pH_{T5} (D) in 5 replicate culture vessels per treatment (\pm SD). Calculated average pCO_2 (E) of 5 replicate culture vessels per treatment (\pm SD). doi:10.1371/journal.pone.0052448.g002

Station (Table 1); for example, this culture developed to early pluteus 4 days faster. As water temperatures within our culturing system were slightly elevated relative to water temperatures reported in Bosch *et al.* [23], the overall faster rate of development

is to be expected; additionally differences between culturing conditions (vessel size and water movement) can result in different developmental rates [23]. Early cleavages, from fertilization to morula stage, (Fig. 3A–C) proceeded normally in all treatments with no obvious morphological or developmental delays between treatments. In addition to the hatching times listed in Table 1, our reported hatching time is intermediate between those observed by Bosch *et al.* [23] for embryos hatched in a seawater table and in a refrigerator (122–110 hrs). As development proceeded, the prolonged transition of mesenchyme blastula to early gastrula provided multiple days to observe changes, such as the gradual formation of the archenteron and the spicule nuclei (Fig. 3D–L). The appearance of the spicule nuclei in the mesenchyme blastula stage (day 8, Fig. 3D–E) was synchronous in all treatments. Early spicule growth appeared similar between treatments (Fig. 3G–I) in the mid-gastrula stage, where the triradiate spicules were extending along all three axes on both sides of the embryo symmetrically.

However, as development proceeded to the late gastrula stage (day 12), the lengthening of the spicules was not the same between treatments (Fig. 3J–L, see also below). Some aberrant development, both in gross morphology and skeletal elements, was observed in elevated CO_2 treatments from late gastrula and prism (Fig. 3L, Fig. 4B–C), though these abnormal individuals constituted only a small proportion (see below). Abnormalities included underdeveloped or highly asymmetric skeletal elements and signs of developmental arrest in gross morphology. At sampling on day 20, developmentally arrested larvae were no longer observed in cultures. Gross morphology of plutei appeared normal as canonical 4-arm echinoplutei, across treatments with no signs of increased asymmetry (Fig. 4D–I). The shapes of most skeletons in prisms (Fig. 4A–C) and plutei (Fig. 4D–I) were normal in all treatments even though the arms were visibly shorter in the high pCO_2 treatments. Spicule nuclei of the posterodorsal arms (Fig. 4G

Table 1. Developmental schedule (days post-fertilization) of *S. neumayeri* reared in water from McMurdo Sound – for this study and for data reported by Bosch *et al.* [23].

Stage	This study		
	–0.8 to 0°C	–0.5 to +0.5°C*	–1.8 to –0.9°C
4-cell	0.7		
8-cell	1.0		
Early blastula	2.0	1.7	2.1
Early blastula with cilia	3.2		
Unhatched motile blastula	4.1		
Hatching	4.7	3.7	5.1
Mesenchyme (M) blastula	5.3		
Early gastrula ⁵ with spicule	7.9	8	10
Mid-gastrula	8.8		
Late gastrula	9.3		
Stomatodeal breakthrough	12		
Prism	15	15	16
Early 4-arm pluteus	17	17	21

They have reported the first appearance of stages while our report is the stage of the majority of embryos observed.

*Cultures grown in Santa Cruz, CA, USA.

⁵The indentation of the vegetal plate was initiated but the archenteron was not yet formed. See also Fig. 3F.

doi:10.1371/journal.pone.0052448.t001

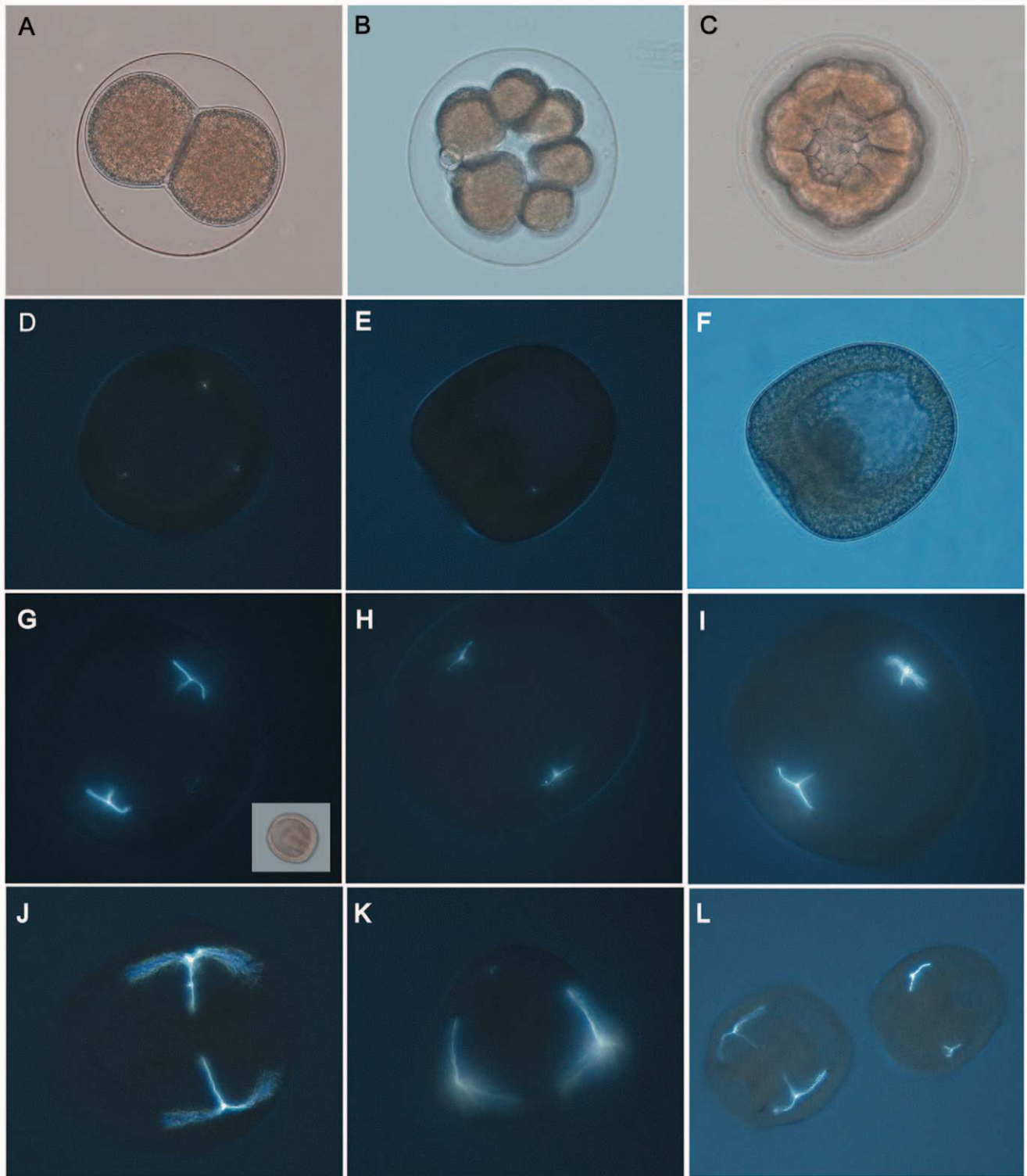


Figure 3. Developmental series of embryo images, including polarized microscopy. Developmental stages and skeletal development of *S. neumayeri* under elevated pCO₂. A–C) Representative embryos at 2 cell, 16 cell and morula stages reared under ambient (unmanipulated seawater) conditions in a separate culture. D–F) Eight day old early gastrula with vegetal plate indentation where CaCO₃ spicule nuclei are first visible. Three spicule nuclei are visible under polarized light (D) from the ventral view of the embryo grown in the control treatment. Polarized (E) and brightfield (F) side views of a gastrula grown in 730 μatm pCO₂ treatment. Two spicule nuclei among the mesenchyme cells are visible from this angle. G–I) Ten day old mid-gastrula embryos (also G-inset) from three treatments: control (G), 510 μatm (H) and 730 μatm (I). Triradiate spicules are similar in shape. J–L) Twelve day old late gastrula stage embryos in three treatments. Large well-developed spicules are visible from the side (J, L) and ventral view (K). Aberrant spicule development is readily distinguishable in some individuals in the 730 μatm treatment (L). doi:10.1371/journal.pone.0052448.g003

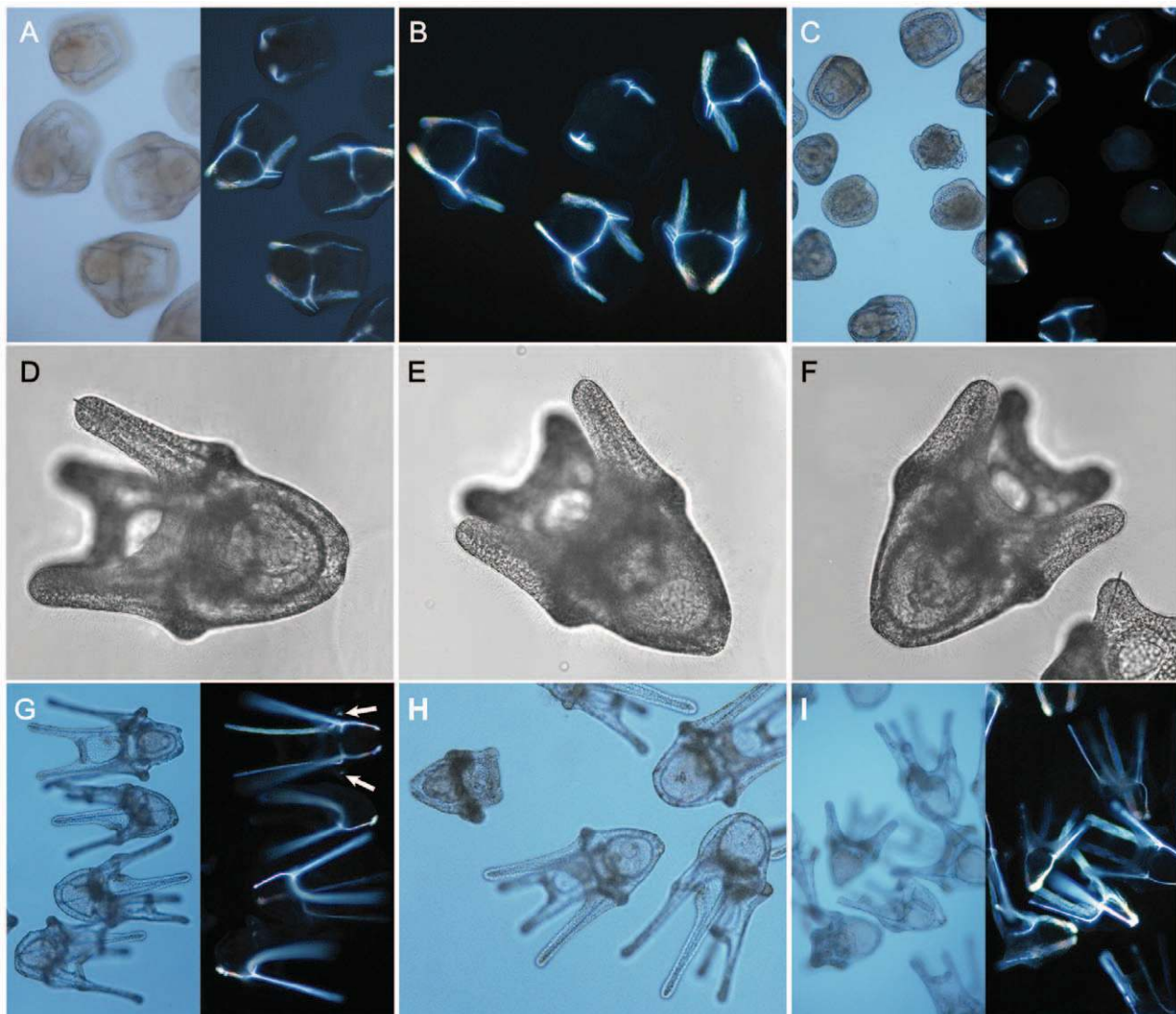


Figure 4. Developmental series of larvae images, including polarized microscopy. A–C) Fifteen day old prism larvae imaged under brightfield and polarized light. Aberrant skeletal and morphological development is found in the 510 μatm (B) and 730 μatm (C) treatments. D–F) Twenty day old 4-arm plutei in three treatments as imaged for morphometric measurements. G–I) Thirty day old plutei. Spicule nuclei for the developing posterodorsal arms are visible in the polarized light image of control treatment larvae (G-arrow). Smaller larvae with short arms are visible in the 510 μatm and 730 μatm treatments (H, I).
doi:10.1371/journal.pone.0052448.g004

- arrow) were visible in some individuals at all treatment levels but were most apparent in the control.

Developmental Staging

Fixed larvae were quantitatively staged over development to look for evidence of developmental delay resulting from elevated pCO₂ (Fig. 5). In general we observed similar (and not significantly delayed) developmental progression at almost every major developmental stage sampled. Embryos at day 1 showed the greatest variation in cell divisions (Fig. 5A), from 2-cell to 16-cell with elevated pCO₂ treatments developing slightly faster than controls (Fisher's exact test, $p < 0.01$); at later stages (Fig. 5B–E), stage differences were more subtle and there appeared to be more synchrony. One consistently observed (but rare) abnormality in early embryos was premature loss of the fertilization envelope; this was scored separately at day 2 as “no fertilization membrane early blastula” (no FM-E Blas), as distinct from early blastulas with the

fertilization membrane intact (E Blas: Fig. 5B). A small percentage of abnormally developed larvae were observed in all treatments throughout development, but there were no differences between treatments (Fisher's exact test on proportions of abnormal embryos over time: $df = 29$, $p > 0.9$) (Fig. 5F).

Unhatched blastulas without cilia (UH-no cilia Blas: Fig. 5C) on day 3 were similar to the stage E Blas on day 2. The hatching of blastulas at day 5 was differentiated somewhat between treatments (Fig. 5C). On day 4 prior to hatching, ciliated, motile blastulas were observed in the culture (Table 1). At day 5, earlier-stage blastulas were unhatched but ciliated (UH+cilia Blas-inset left) or hatched (H Blas). Mesenchyme blastulas with a distinct vegetal plate and animal-vegetal patterning were observed with fertilization membranes (UH Mes Blas) in the 510 and 730 μatm treatments suggesting delayed hatching relative to remaining blastulas (H Mes Blas). Analysis with Fisher's exact test is highly significant ($p < < 0.001$) for stage differences at day 5.

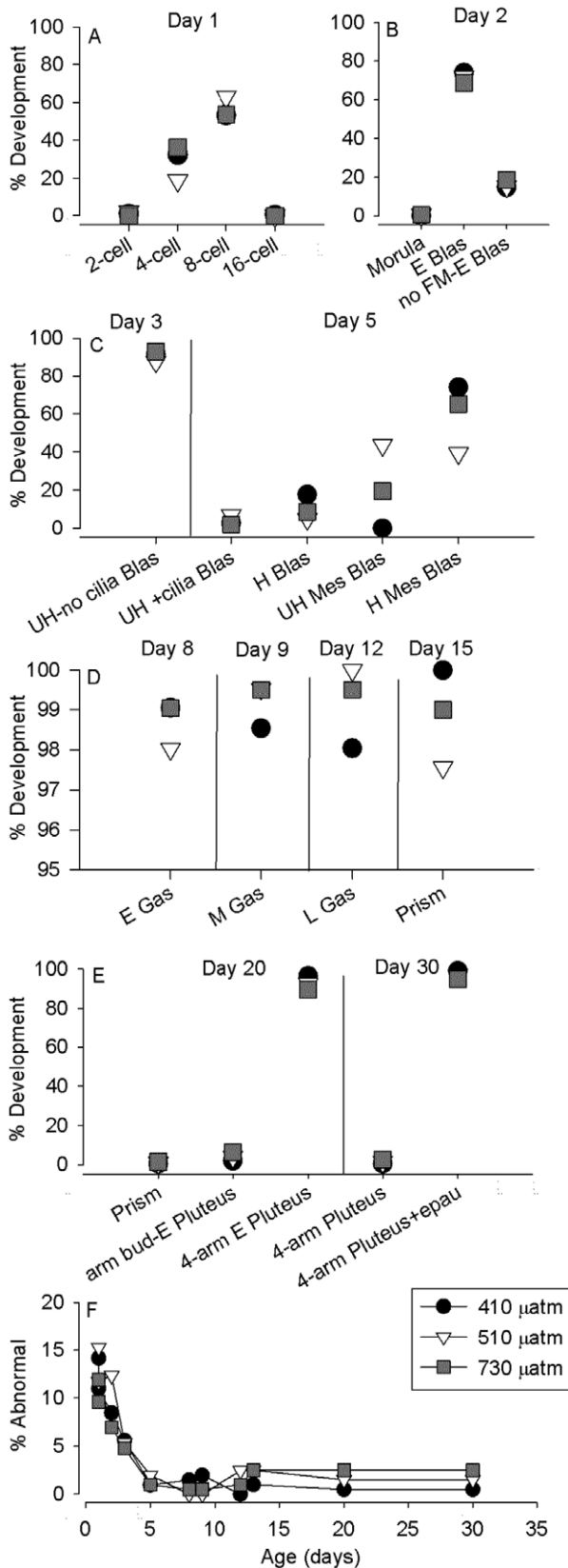


Figure 5. Developmental progression and synchrony at specific times over the duration of the experiment. Samples for each specified day (n>200, each treatment) were scored for developmental stage. A) Relative percentages of normally developed 2–16 cell embryos

at 1 day post-fertilization. B) Relative percentages of morulas, and early blastulas (E Blas) at Day 2. Some normally developed embryos were missing a fertilization membrane (no FM-E Blas). C) Day 3 and 5 development. Unhatched (UH) blastulas were observed without cilia (UH-no cilia Blas) on day 3, while ciliated blastulas in various stages were observed at Day 5. Earlier-stage blastulas were unhatched but ciliated (UH+cilia Blas-inset left) or hatched (H Blas). More developed mesenchyme blastulas (Mes Blas) with a distinct vegetal plate were also unhatched and hatched (inset right). D) Gastrulation over days 8–15. Note the change in Y-axis scale. Early gastrula (E Gas) mid-gastrula (M Gas) late gastrula (L Gas) and prism were observed in highly synchronous development. E) Pluteus development at days 20 and 30. Prism and early pluteus (E Plu) were observed at day 20. By day 30 the 4-arms of the plutei are well-developed and some have developed epaulettes (+epau). F) Abnormal development across the experimental period. Percentage of unfertilized and abnormally developed embryos and larvae are shown for the three pCO₂ treatments. doi:10.1371/journal.pone.0052448.g005

Gastrula development, from days 8 to 12 was largely synchronous between treatments (Fisher’s exact tests for each sampling day, p>0.05) (Fig. 5D). Indentation at the vegetal pole was the characteristic of early gastrula (E Gas) at day 8, and archenterons halfway extended (mid-gastrula, M Gas) and fully extended (late gastrula, L Gas) were observed in samples from day 9 and 12 respectively. There was a single “unhatched mid-gastrula” at day 9 observed in the 510 μatm treatment [M. Sewell, pers. obs.].

In early plutei at day 20 (Fig. 5E) there was differentiation of external features such as arm buds (arm bud-E Plu) vs. more clearly developed arms (4-arm E Plu). Because larvae were unfed in this experiment, developmental progression was drastically slowed, though arm extension and the appearance of other morphological characters continued. In later plutei at day 30, epaulettes, thickened lobes of ciliated band epithelium on the body that have elongated cilia [23], were observed on the majority of plutei (4-arm pluteus+epau): an indication of continued larval maturation in the absence of food. Differences at prism and pluteus stages were not significant between pCO₂ treatments (Fisher’s exact tests for each sampling day, p>0.05).

Morphometrics

In order to quantify the size differences between treatments, the embryos and larvae were measured on their largest, most readily quantifiable metrics for their developmental stage: the ALA rod for embryos, and TL (and POA and body rods where applicable) for pluteus (see Fig. 1). Because variances were highly unequal between treatments at most sample points, PERMANOVA, a permutation-based ANOVA was implemented due to its insensitivity to both non-normality and heteroscedasticity (Table 2). Dispersion of measurements was significantly heterogeneous in late gastrulae at day 12 (p<0.004) between treatments, but homogeneous at all other stages. Lengths of both skeletal elements and larvae were significantly different between treatments at all stages. At day 12 the 510 μatm treatment was significantly larger than the control 410 μatm treatment (Fig. 6A, Table 2). In the prism (day 15) stage, the ALA rods were significantly shorter in the 730 μatm treatment (Fig. 6A, Table 2); the differences between 410 and 730 μatm treatments were significant in every measurement from day 15 onward.

By the pluteus stage, the total lengths of the larvae were consistently smaller in the 730 μatm treatment than in the control 410 μatm treatment (Fig. 6B, Table 2). Only at day 20 were the 510 μatm treatment larvae more similar to 730 μatm than to 410 μatm, while the day 30 measurements show no significant difference between 410 and 510 μatm treatment larvae in lengths.

Table 2. Permutational homogeneity of dispersion (PERMDISP2), PERMANOVA and permutational pairwise statistics on morphometrics data.

Age	Measurement	Permutational dispersion (PERMDISP2)	PERMANOVA p	Pairwise tests between treatments
12	Anterolateral arm (ALA) rod length	0.004**	0.005**	730<510 410=730 410=510
15	ALA rod length	NS	0.037*	730<410 410=510 510=730
20	Total length	NS	0.001**	730<410 510<410 510=730
30	Total length	NS	0.001**	730<410 730<510 410=510
30	Postoral (POA) arm rod length	NS	1×10 ⁻⁴ ***	730<410 730<510 410=510
30	Body rod length	NS	1×10 ⁻⁴ ***	730<410 730<510 410=510

doi:10.1371/journal.pone.0052448.t002

At day 30, these total length differences in the 730 μatm treatment were primarily the result of arm length differences (see also Fig. 7), though both arm and body rod lengths were shorter than both control and 510 μatm larvae. The percent contribution of arm length to total larval length was significantly less at 730 μatm (ANOVA, $p < 0.001$) than at lower pCO₂ levels (56.1% vs 68–69%, not shown). Because arm length comprises most of total larval length the two will always be correlated, but body rod length is less plastic [48].

Allometry of advanced 4-arm plutei was performed on length measurement data to examine the possible differential effects of CO₂ treatments on arm and body size. Individual differences in response between treatments were reflected in different allometric relationships. Allometric analysis on the morphometrics of individual plutei at day 30 (Fig. 7A) shows that there is complete overlap between control 410 and 510 μatm treatments while the 730 μatm treatment is distinct. The differences in variance between treatments in POA and body rod lengths are readily apparent (see also Fig. 6B). Despite the clear overlap in distributions between control and 510 μatm, POA rod length

was significantly related to body rod length ($r^2 = 0.14$, $p < 0.04$) only in the control 410 μatm treatment; the two measures were not significantly related at elevated pCO₂ (Fig. 7A). The low r^2 within all treatments suggests that the ratio of POA to body rod length (POA rod:body rod) is fairly plastic between individuals within a population, even between half-siblings, and this ratio is not significantly different between treatments (ANOVA, $p > 0.6$). Despite the similarities in POA rod:body rod between treatments, only at elevated pCO₂ was there a significant relationship (510 μatm: $r^2 = 0.29$, $p < 0.003$; 730 μatm: $r^2 = 0.32$, $p < 0.002$) between POA rod:body rod and body rod length (Fig. 7B).

Discussion

The near-future potential for year-round calcium carbonate undersaturation in polar oceans indicates that lightly calcified Antarctic invertebrate fauna could be more vulnerable to mildly elevated levels of CO₂ than organisms in warmer marine ecosystems [3,48]. In this study, we investigated the effects of elevated pCO₂ on the larvae of the common benthic echinoderm

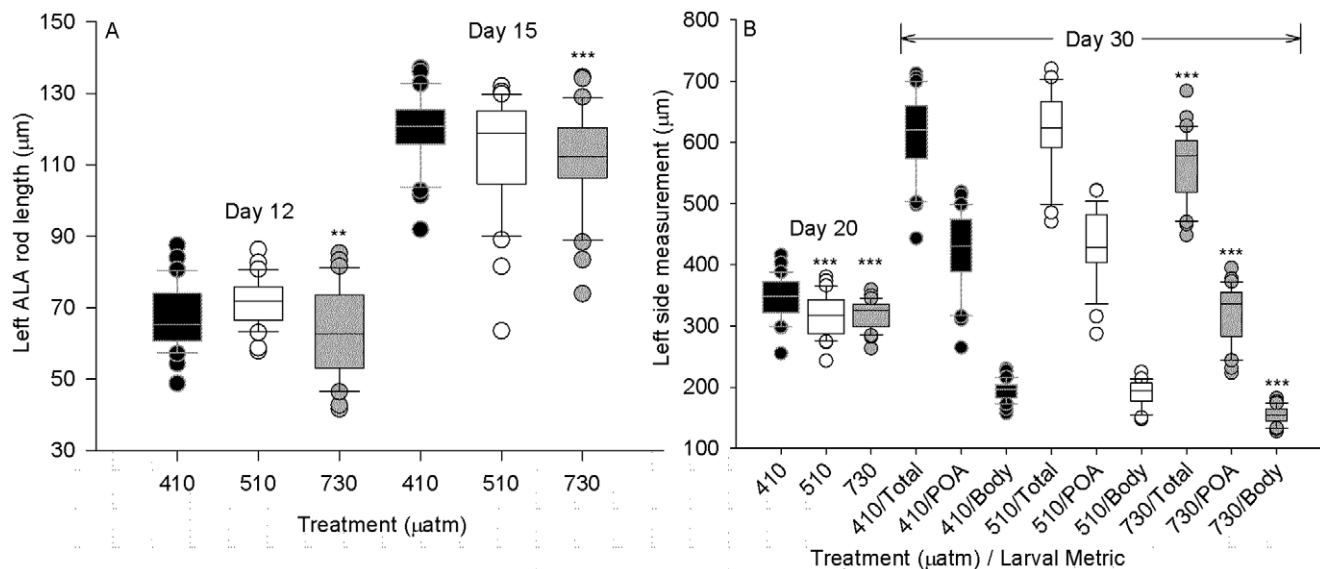


Figure 6. Morphometrics of skeletal elements and larval size from late gastrula to 4-arm pluteus (from day 12–30). Box plots show median, 25th and 75th percentile within the boundaries of the box, 10th and 90th percentiles in the error bars and three lowest and highest outlier values. See Fig. 1 for diagram of measurements. See Tables 1 and 2 for statistics on variances and differences between treatments. A) Anterolateral arm (ALA) rod length (left side) during late gastrulation to prism transition ($n = 30$). B) Total length in early (day 20) and advanced (day 30) 4-arm plutei. Also shown for day 30 plutei are the postoral arm (POA) rod lengths and body rod lengths ($n = 30$, except $n = 29$ for 510 μatm at day 30). doi:10.1371/journal.pone.0052448.g006

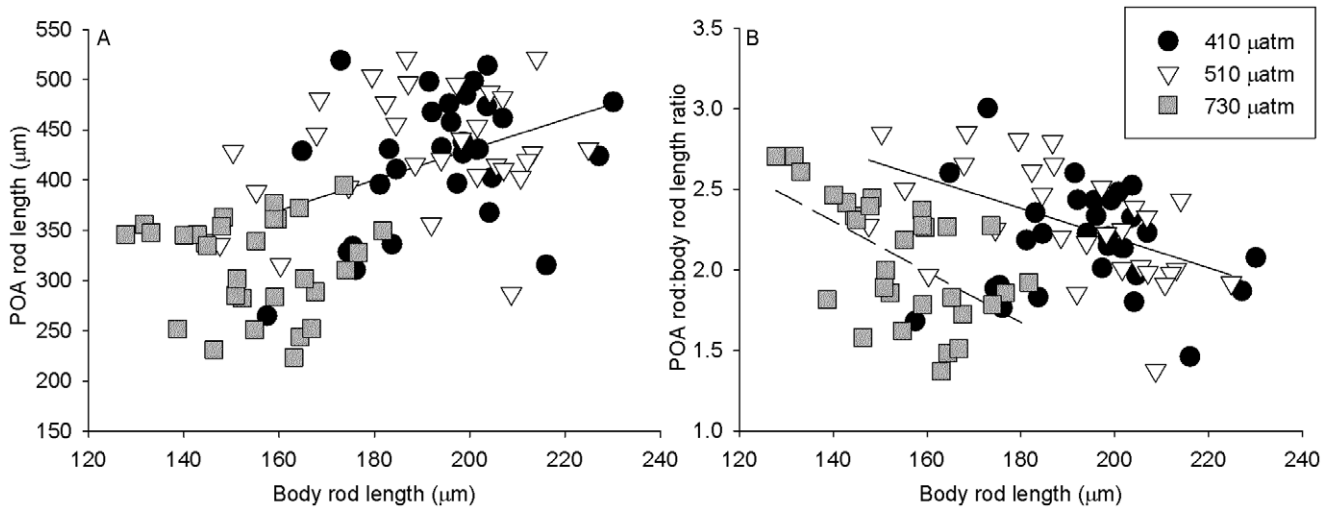


Figure 7. Allometric comparisons of body and arm lengths at day 30. Allometry of individual day 30 plutei considering body rod length as an independent factor. A) The relationship between body rod length and postoral arm (POA) rod length for all assayed individuals in 3 pCO₂ treatments (n=30 for 410 and 730 μatm treatments, n=29 for 510 μatm). POA rod length is correlated significantly to body rod length ($r^2=0.14$, $p<0.04$) only in the control (410 μatm) treatment (solid line; regressions not shown for NS correlations). B) Relationship of body rod length to POA rod:body rod length ratio. There was a significant correlation at 510 μatm (solid line, $r^2=0.29$, $p<0.003$) and at 730 μatm (dashed line, $r^2=0.32$, $p<0.002$). NS correlation for control not shown. doi:10.1371/journal.pone.0052448.g007

Sterechinus neumayeri. Over the course of development from egg to late 4-arm pluteus, we found (1) early embryological development was normal with the exception of the hatching process, which was slightly delayed, (2) the onset of calcification as determined by the appearance of CaCO₃ spicule nuclei was on schedule, (3) the lengths of the spicule elements, and the elongation of the spicule nuclei into the larval skeleton, were significantly shorter in the highest CO₂ treatment 4 days after the initial appearance of the spicule nuclei, (4) finally, without evidence of true developmental delay, larvae were smaller overall under high CO₂ treatments and arm length, the most plastic morphological aspect of the echinopluteus, exhibited the greatest response to high pCO₂/low pH/low carbonate conditions.

Seawater Conditions: in the Field and in the Lab

In order to adequately parameterize the control conditions for our experiment, we sampled seawater from the Cape Evans area to assess present day levels of carbonate chemistry where urchin larvae would be present in the plankton. Current water conditions at McMurdo Sound are already at low Ω_{ara} saturation levels (1.24 at Cape Evans [20]), and Antarctic waters are predicted to become aragonite undersaturated ($\Omega_{\text{ara}} < 1$) in the very near future on a seasonal basis [4,17], and completely undersaturated a few decades thereafter [1,49]. Thus for our experiments we targeted $\sim 400 \mu\text{atm}/\Omega_{\text{ara}}=1.24$ for ambient levels, and $\Omega_{\text{ara}} \approx 1$ and $\Omega_{\text{ara}} < 1$ for our elevated pCO₂ future climate treatments; the discrepancy between culture temperatures and environmental temperatures prevented us from more precisely matching our target values.

We then tested the effects of elevated CO₂ levels on early development of *S. neumayeri* in seawater from McMurdo Sound, and found that embryos and larvae were developmentally robust to the experimental conditions. Rates of survival, while not directly measured, were high in all CO₂ treatments (410, 510 and 730 μatm) over the duration of the experiment. Previous research on larvae of *S. neumayeri* reported survival differences only at very severely lowered pH levels ($\text{pH}_{\text{NBS}} < 6.5$) [29]. Similarly,

deleterious effects during embryonic development were reported only at low pH ($\text{pH}_{\text{NBS}} \leq 7.3$, which would correspond to $\text{pCO}_2 > 2880 \mu\text{atm}$: [13], and $\text{pH}_{\text{TS}} = 7.5$: [30]).

Developmental Progression

In order to address the potential confounding of decreased growth and delayed development, we monitored developmental progression of larvae in order to ascertain whether developmental delays would result from elevated pCO₂ conditions. Developmental scheduling in all CO₂ treatments was similar to previously reported data for this species (Table 1). Because of the warmer temperatures indoors in the Crary Lab (Fig. 2C), cultures could not be consistently maintained at the true environmental temperature of -1.9°C , and as a result, the developmental rate of our embryos was accelerated relative to the rates reported by Bosch *et al.* [23], particularly in comparison to the hatching time reported for embryos cultured *in situ* in McMurdo Sound (5.8 days: [23]).

Early embryos were indistinguishable in appearance between all CO₂ treatment groups, demonstrating a lack of effect on basic cell-division and morphogenesis. One study reported deleterious CO₂ effects on early cell divisions only at sub-optimal sperm concentrations [13]; other evidence demonstrates an overall negative effect of elevated pCO₂ but that responses can be variable between male-female pairs [50]. Elevated temperature has deleterious effects on early cleavages [51], but not with synergistic effects of low pH [30]. Another study on the possible mechanism of delays at first cleavage in *Strongylocentrotus purpuratus* under highly elevated CO₂/low pH (pH 7.0/4000 ppm pCO₂) demonstrated no deleterious effects on cell cycle checkpoints [52]. Developmental progression from early blastula to mesenchyme blastula in *S. neumayeri* was similar between treatments but hatching rates were not. Differences in development were most obvious at day 5, the hatching blastula stage (Fig. 5C). There have not been previous reports regarding the effects of CO₂ on hatching, but research on enzymatic activity of purified hatching proteases from temperate sea urchin species suggest that pH 8 is

optimum for maximal activity *in vitro* [53,54]. Though hatching was delayed, the embryos developed on schedule within the envelope, which suggests a decoupling of the hatching process from the other more critical developmental pathways; echinoid embryonic development can proceed normally in the absence of a fertilization envelope in culture and the removal of the envelope is required for techniques such as blastomere separation [55,56]. Delayed hatching with developmental progression in echinoids has now been reported as a response to salinity stress [57], so our observation of delayed hatching is perhaps indicative of an environmental stress response.

Developmental progress was synchronous from gastrulation onward with non-significant differences in developmental staging between treatments over the course of development to pluteus. Gastrulation is a critical developmental regulation point [58] at which major gene expression changes can also result in mortality due to genetic load in high fecundity invertebrates [59,60]. Low percentage of gastrulation abnormalities at mildly elevated pCO₂ treatments is consistent with previous reports in *S. neumayeri* (for pH_{NBS} ≥ 7.7: [13]), and in *Strongylocentrotus purpuratus* [61]. Gastrulae and larvae with skeletal anomalies (of the varieties seen in Fig. 3L, Fig. 4B and C) were observed in all treatments (Fig. 5F). Studies in *Strongylocentrotus purpuratus* have failed to detect delays in the spicule nuclei appearance prior to skeleton elongation under elevated pCO₂ [61], and control over spiculogenesis and the initial precipitation of these CaCO₃ nuclei is distinct from spicule elongation processes in the primary mesenchyme cells [62,63].

Morphometric Differences

The significantly smaller larvae observed in the 730 μatm treatment are consistent with observations of less growth under elevated CO₂/low pH in the larvae many other species of sea urchin when tested under future climate scenarios [35,37,39,64]. However while the pCO₂ treatment level (730 μatm) which has effected this difference (~8% at all 4 measured stages) is much lower than has been used with experiments on temperate larvae (compare with effects at 1000 μatm in *Strongylocentrotus purpuratus*: [65]), the Ω_{ara} difference tested on the polar species is smaller and going from saturation (Ω_{ara} = 1.35) to undersaturation (Ω_{ara} = 0.82). The Antarctic species appears to respond with greater sensitivity than temperate species to smaller changes in pCO₂/pH/Ω because it currently lives in conditions that are already difficult for calcification. The use of Ω_{ara} rather than Ω_{cal} for comparison is appropriate due to the Mg⁺² content of calcite deposited by echinoderms [5,66].

The size difference between treatments in ALA rods at late gastrulation shows that the differences are detectable early in the skeleton development process, even though there was no substantial delay in the first appearance of the initial spicule nuclei between treatments. Differences in size of the POA rod at day 30 show that the differences in total length are largely attributable to POA length differences. This finding is unsurprising given that arm length is the most plastic attribute of echinopluteus larvae, and can be readily modified in response to food cues [67,68,69,70] and pharmacological manipulation [71]. Recent studies [72,73] have asserted that developmental delay is solely responsible for the smaller size of larvae under elevated CO₂. Because the plasticity of the feeding arms in echinoid larvae is controlled by food and hormonal cues [70,71,74] arm length may not represent a reliable “fixed” metric from which to determine relative age.

The skeletal elements of larvae are significantly and consistently smaller in the 730 μatm treatment at days 15 and 30. While there were overall significant length differences between treatments at day 12, the significant dispersion (as tested by PERMDISP)

appears to be between the two elevated pCO₂ treatments, and greater size variance at elevated pCO₂ has been observed in other sea urchin larvae [75]. If a delay and/or slower growth had occurred to make larvae at high CO₂ smaller, this difference may have occurred subsequent to the earliest growth period after day 12. Body rod length does not appear to increase in this species after the attainment of the pluteus in the absence of food [P. Yu, unpub.], as reported in some other species of echinoid [47,74]. The smaller body rod size of advanced 4-armed larvae in *S. neumayeri* suggests that smaller body size under high pCO₂ is not a growth intermediate, but could either be fixed at attainment of the pluteus stage at a smaller size, or even be the result of shrinkage during food deprivation. The allometric changes in response to elevated pCO₂ (Fig. 7A: loss of correlation between POA rod and body rod lengths and Fig. 7B: increasing response of the POA: body rod ratio to body rod length) is also suggestive of true size changes imposed by elevated pCO₂ as delayed growth would not result in a relaxation of allometric relationships. Larval growth is regulated by cell number, not cell size [76], so future measurements of cell number in this species may clarify some of the observed differences. The simultaneous interaction of growth and development in continuously growing invertebrate larvae is still poorly understood, as compared with the amount of knowledge in arthropods regarding size-age relationships [77].

Physiological Implications of Size Differences

Due to the simultaneous interaction of growth and development, the effect of slower growth vs. age-delay cannot be readily decoupled developmentally or mechanistically without additional markers of developmental progression in continuously growing larvae [78]. Interpretations of a developmental delay mechanism based on decreased metabolism are inconclusive, as a previous study on metabolic rates in larvae of *S. neumayeri* suggested a decreased metabolic rate under elevated pCO₂ [79] while in temperate species, size-specific metabolic rates were unchanged [73] or increased [72]. There was no evidence for developmental delay from developmental staging [80] or rates of lipid catabolism [81] under elevated pCO₂ in *Strongylocentrotus purpuratus* during early development. Gene expression patterns under elevated CO₂ during early development showed no differences that would indicate developmental delay [82], while other studies have interpreted their results as indicative of developmental delay [83]. The synchrony of overall development observed in our cultures between treatments (Fig. 5) provides strong evidence for a lack of developmental delay and for attenuation in size due to lower growth.

Arm length is important for maintaining buoyancy during swimming and for food capture in echinoplutei. Maintaining longer arms involves growth trade-offs [84], and longer arms correlate with ciliated band length and feeding capacity [84], and organismal lipid content [71,81]. Though elevated CO₂ has been repeatedly shown to result in shorter arm lengths, data from Stumpp *et al.* [72] show that size-specific feeding rates are not affected by pH treatment. While we elected to not feed the larvae in this study, the early development of these larvae in their environment during the late austral spring is under nutrient-poor conditions [41]; thus our experimental conditions represent a temporary natural stress for the larvae. Studies on later, more advanced larval development would need to incorporate naturalistic feeding treatments to better ascertain the downstream developmental effects of smaller arm and body size. Studies on juvenile corals have shown that feeding can mitigate some of the effects of low pH on growth and calcification (reviewed in [85]),

but the correlation of arm length to feeding in echinoid larvae means that shorter arms from high pCO₂ will inhibit food intake.

Slower growth and smaller size could lead to longer pelagic larval duration, which for *S. neumayeri* is almost 4 months under optimal conditions [23]. Spawning of *S. neumayeri* is timed slightly in advance of seasonal availability of phytoplankton resources [86], and phenological mismatch during development could potentially occur with climate change. Longer pelagic larval duration can also result in increased pelagic predation risk [87,88]. Recruitment of *S. neumayeri* is estimated to be sporadic and low, suggesting most annual gonadal production is already consumed by predators [89].

The Ross Sea currently faces a number of environmental challenges. Estimates of future undersaturation are only a few decades away by the most recent model estimates [4]. A slight increase in pCO₂ (+100 μ atm above present day levels) did not consistently decrease size in this species over most of early larval development. Notably, an elevation of pCO₂ by about twice current atmospheric levels (projected to occur by the year 2050: [49]) resulted in significantly smaller skeletons and bodies, but did not noticeably change rates of early development in a slow-growing species. Future warming will accelerate development times, but may then result in undersized larvae with simultaneously elevated pCO₂ conditions. Based on demographic surveys,

the lifespan of *S. neumayeri* is estimated to be roughly 40 years in the McMurdo Sound region [89], making the settlers of the present day the highest fecundity reproductive classes of these future acidified conditions. Currently in parts of the Antarctic Peninsula, predation on adult urchins by invasive crabs present a more immediate threat to this species [8,9]. Thus there will be a multitude of simultaneous challenges to the future persistence of this species and other shelled invertebrates of Antarctica.

Acknowledgments

The authors would like to thank members of the U.S. Antarctic Program: C. Sucher, P. McMillan, J. Watson, R. Robbins and S. Rupp for technical support and animal collection at McMurdo Station, Antarctica. PCY would especially like to thank J. Janoso of Northern Focus for his advice and technical support. We thank E. Hunter from the Bravo 134 field team for his support during larval culture and water chemistry measurements. The authors are grateful to Dr. J. Dutton for assistance with water chemistry data management.

Author Contributions

Conceived and designed the experiments: PCY MAS GEH. Performed the experiments: PCY MAS PGM EBR LK GEH. Analyzed the data: PCY MAS. Wrote the paper: PCY MAS GEH.

References

1. Feely RA, Doney SC, Cooley SR (2009) Ocean Acidification: Present Conditions and Future Changes in a High-CO₂ World. *Oceanography* 22: 36–47.
2. Orr JC, Fabry VJ, Aumont O, Bopp L, Doney SC, et al. (2005) Anthropogenic ocean acidification over the twenty-first century and its impact on calcifying organisms. *Nature* 437: 681–686.
3. Fabry VJ, McClintock JB, Mathis JT, Grebmeier JM (2009) Ocean Acidification at High Latitudes: The Bellweather. *Oceanography* 22: 160–171.
4. McNeil BI, Matear RJ (2008) Southern Ocean acidification: A tipping point at 450-ppm atmospheric CO₂. *P Natl Acad Sci USA* 105: 18860–18864. 10.1073/Pnas.0806318105.
5. Andersson AJ, Mackenzie FT, Bates NR (2008) Life on the margin: implications of ocean acidification on Mg-calcite, high latitude and cold water marine calcifiers. *Mar Ecol Prog Ser* 373: 265–273. 10.3354/meps07639.
6. McClintock JB, Angus RA, McDonald MR, Amsler CD, Catledge SA, et al. (2009) Rapid dissolution of shells of weakly calcified Antarctic benthic macroorganisms indicates high vulnerability to ocean acidification. *Antarct Sci* 21: 449–456. 10.1017/S0954102009990198.
7. Sewell MA, Hofmann GE (2011) Antarctic echinoids and climate change: a major impact on the brooding forms. *Global Change Biol* 17: 734–744. 10.1111/j.1365-2486.2010.02288.x.
8. Smith CR, Grange IJ, Honig DL, Naudts L, Huber B, et al. (2012) A large population of king crabs in Palmer Deep on the west Antarctic Peninsula shelf and potential invasive impacts. *Proc Roy Soc B: Biol Sci* 279: 1017–1026. 10.1098/rspb.2011.1496.
9. Thatje S, Hall S, Hauton C, Held C, Tyler P (2008) Encounter of lithodid crab *Paralomis birsteini* on the continental slope off Antarctica, sampled by ROV. *Polar Biol* 31: 1143–1148. 10.1007/s00300-008-0457-5.
10. Aronson RB, Thatje S, Clarke A, Peck LS, Blake DB, et al. (2007) Climate Change and Invasibility of the Antarctic Benthos. *Annu Rev Ecol Evol S* 38: 129–154. 10.1146/annurev.ecolsys.38.091206.095525.
11. Cummings V, Hewitt J, Van Rooyen A, Currie K, Beard S, et al. (2011) Ocean Acidification at High Latitudes: Potential Effects on Functioning of the Antarctic Bivalve *Laternula elliptica*. *PLoS ONE* 6: e16069. 10.1371/journal.pone.0016069.
12. Kawaguchi S, Kurihara H, King R, Hale L, Berli T, et al. (2011) Will krill fare well under Southern Ocean acidification? *Biol Letters* 7: 288–291. 10.1098/rsbl.2010.0777.
13. Ericson JA, Lamare MD, Morley SA, Barker MF (2010) The response of two ecologically important Antarctic invertebrates (*Stereochinus neumayeri* and *Parborlasiastis corrugatus*) to reduced seawater pH: effects on fertilisation and embryonic development. *Mar Biol* 157: 2689–2702. 10.1007/S00227-010-1529-Y.
14. Seibel BA, Maas AE, Dierssen HM (2012) Energetic Plasticity Underlies a Variable Response to Ocean Acidification in the Pteropod, *Limacina helicina antarctica*. *PLoS ONE* 7: e30464. 10.1371/journal.pone.0030464.
15. Lebrato M, Iglesias-Rodriguez D, Feely RA, Greeley D, Jones DOB, et al. (2010) Global contribution of echinoderms to the marine carbon cycle: CaCO₃ budget and benthic compartments. *Ecol Monogr* 80: 441–467. 10.1890/09-0553.1.
16. Brey T, Gutt J (1991) The genus *Stereochinus* (Echinodermata: Echinoidea) on the Weddell Sea shelf and slope (Antarctica): distribution, abundance and biomass. *Polar Biol* 114: 227–232. 10.1007/BF00238455.
17. McNeil BI, Tagliabue A, Sweeney C (2010) A multi-decadal delay in the onset of corrosive ‘acidified’ waters in the Ross Sea of Antarctica due to strong air-sea CO₂ disequilibrium. *Geophys Res Letters* 37. L19607. 10.1029/2010gl044597.
18. Yoshikawa-Inoue H, Ishii M (2005) Variations and trends of CO₂ in the surface seawater in the Southern Ocean south of Australia between 1969 and 2002. *Tellus B* 57: 58–69. 10.1111/j.1600-0889.2005.00130.x.
19. Sabine CL, Feely RA, Wanninkhof R, Dickson AG, Millero FJ, et al. (2012) Carbon Dioxide, Hydrographic, and Chemical Data Obtained During the R/V Nathaniel B. Palmer Cruise in the Southern Ocean on CLIVAR Repeat Hydrography Section S04P (Feb. 19 - Apr. 23, 2011). Oak Ridge, TN, USA: Carbon Dioxide Information Analysis Center, Oak Ridge National Laboratory, US Department of Energy.
20. Matson PG, Martz TR, Hofmann GE (2011) High-frequency observations of pH under Antarctic sea ice in the southern Ross Sea. *Antarct Sci* 23: 607–613. 10.1017/S0954102011000551.
21. Martz TR, Connery JG, Johnson KS (2010) Testing the Honeywell Durafet (R) for seawater pH applications. *Limnol Oceanogr-Methods* 8: 172–184. 10.4319/lom.2010.8.172.
22. Hofmann GE, Smith JE, Johnson KS, Send U, Levin LA, et al. (2011) High-Frequency Dynamics of Ocean pH: A Multi-Ecosystem Comparison. *PLoS ONE* 6: e28983. 10.1371/journal.pone.0028983.
23. Bosch I, Beauchamp KA, Steele ME, Pearse JS (1987) Development, metamorphosis, and seasonal abundance of embryos and larvae of the Antarctic sea-urchin *Stereochinus neumayeri*. *Biol Bull* 173: 126–135.
24. Clarke A, Johnston NM, Murphy EJ, Rogers AD (2007) Introduction. Antarctic ecology from genes to ecosystems: the impact of climate change and the importance of scale. *Philos T R Soc B-Biol Sci* 362: 5–9. 10.1098/rstb.2006.1943.
25. Peck LS, Morley SA, Clark MS (2010) Poor acclimation capacities in Antarctic marine ectotherms. *Mar Biol* 157: 2051–2059. 10.1007/s00227-010-1473-x.
26. Fabry VJ, Seibel BA, Feely RA, Orr JC (2008) Impacts of ocean acidification on marine fauna and ecosystem processes. *ICES J Mar Sci* 65: 414–432. 10.1093/icesjms/fsn048.
27. Comeau S, Jeffree R, Teysseie JL, Gattuso J-P (2010) Response of the Arctic Pteropod *Limacina helicina* to Projected Future Environmental Conditions. *PLoS ONE* 5: e11362. 10.1371/journal.pone.0011362.
28. Comeau S, Gorsky G, Jeffree R, Teysseie JL, Gattuso JP (2009) Impact of ocean acidification on a key Arctic pelagic mollusc (*Limacina helicina*). *Biogeosciences* 6: 1877–1882. 10.5194/bg-6-1877-2009.
29. Clark D, Lamare M, Barker M (2009) Response of sea urchin pluteus larvae (Echinodermata: Echinoidea) to reduced seawater pH: a comparison among a tropical, temperate, and a polar species. *Mar Biol* 156: 1125–1137. 10.1007/S00227-009-1155-8.
30. Ericson J, Ho M, Miskelly A, King C, Virtue P, et al. (2012) Combined effects of two ocean change stressors, warming and acidification, on fertilization and early

- development of the Antarctic echinoid *Sterechinus neumayeri*. *Polar Biol* 35: 1027–1034. 10.1007/s00300-011-1150-7.
31. Leong PKK, Manahan DT (1999) Na⁺/K⁺-ATPase activity during early development and growth of an Antarctic sea urchin. *J Exp Biol* 202: 2051–2058.
 32. Pace DA, Manahan DT (2007) Cost of protein synthesis and energy allocation during development of Antarctic sea urchin embryos and larvae. *Biol Bull* 212: 115–129.
 33. Marsh AG, Maxson REJ, Manahan DT (2001) High macromolecular synthesis with low metabolic cost in Antarctic sea urchin embryos. *Science* 291: 1950–1952.
 34. Marsh AG, Leong PKK, Manahan DT (1999) Energy metabolism during embryonic development and larval growth of an Antarctic sea urchin. *J Exp Biol* 202: 2041–2050.
 35. Kurihara H (2008) Effects of CO₂-driven ocean acidification on the early developmental stages of invertebrates. *Mar Ecol Prog Ser* 373: 275–284. 10.3354/meps07802.
 36. Dupont S, Thorndyke MC (2009) Impact of CO₂-driven ocean acidification on invertebrates early life-history – What we know, what we need to know and what we can do. *Biogeosciences Discuss* 6: 3109–3131. 10.5194/bgd-6-3109-2009.
 37. Byrne M (2011) Impact of ocean warming and ocean acidification on marine invertebrate life history stages: vulnerabilities and potential for persistence in a changing ocean. In: Gibson RN, Atkinson RJA, Gordon JDM, editors. *Oceanography and Marine Biology: An Annual Review*, Vol 49. Boca Raton: Crc Press-Taylor & Francis Group. 1–42.
 38. Jimmy RA, Kelly MS, Beaumont AR (2003) The effect of diet type and quantity on the development of common sea urchin larvae *Echinus esculentus*. *Aquaculture* 220: 261–275. 10.1016/S0044-8486(02)00193-x.
 39. Dupont S, Ortega-Martínez O, Thorndyke MC (2010) Impact of near-future ocean acidification on echinoderms. *Ecotoxicology* 19: 449–462. 10.1007/s10646-010-0463-6.
 40. Fangué NA, O'Donnell MJ, Sewell MA, Matson PG, MacPherson AC, et al. (2010) A laboratory-based, experimental system for the study of ocean acidification effects on marine invertebrate larvae. *Limnol Oceanogr-Methods* 8: 441–452. 10.4319/lom.2010.8.441.
 41. Rivkin RB (1991) Seasonal Patterns of Planktonic Production in McMurdo Sound, Antarctica. 31: 5–16. 10.1093/icb/31.1.5.
 42. Dickson AG, Sabine CL, Christian JR, editors (2007) *Guide to best practices for ocean CO₂ measurements*. Sidney, BC, Canada: North Pacific Marine Science Organization (PICES). 191 p.
 43. Robbins LL, Hansen ME, Kleypas JA, Meylan SC (2010) CO₂calc—A user-friendly seawater carbon calculator for Windows, Max OS X, and iOS (iPhone). In: Survey USG, editor. St. Petersburg, FL. 17.
 44. Wray GA, Kitazawa C, Miner B (2004) Culture of echinoderm larvae through metamorphosis. In: Ettensohn CA, Wessel GM, Wray GA, editors. *Method Cell Biol* 74. Amsterdam, The Netherlands: Elsevier Academic Press. 75–86.
 45. Anderson MJ (2001) A new method for non-parametric multivariate analysis of variance. *Austral Ecol* 26: 32–46.
 46. Oksanen J, Blanchet FG, Kindt R, Legendre P, O'Hara RB, et al. (2011) *vegan: Community Ecology Package*. R package. version 1.17–9 cd.
 47. Anderson MJ (2006) Distance-based tests for homogeneity of multivariate dispersions. *Biometrics* 62: 245–253.
 48. Bougis P (1967) Utilisation des plûtéus en écologie expérimentale. *Helgoland Wiss Meer* 15: 59–68. 10.1007/bf01618609.
 49. Intergovernmental Panel on Climate Change (IPCC) (2007) *Climate Change 2007: The Physical Science Basis, Contribution of Working Group I to the Fourth Assessment Report of the Intergovernmental Panel on Climate Change*; Solomon S, Qin D, Manning M, Chen Z, Marquis M et al., editors. Cambridge, United Kingdom: Cambridge University Press. 987 p.
 50. Sewell MA, Yu PC, Kapsenberg L, Hofmann GE (2011) Ocean Acidification and Sea Urchin Fertilization: A Cautionary Tale with the Antarctic Sea Urchin *Sterechinus neumayeri*. 6th North American Echinoderms Conference. Anacortes, WA.
 51. Stanwell-Smith D, Peck LS (1998) Temperature and Embryonic Development in Relation to Spawning and Field Occurrence of Larvae of Three Antarctic Echinoderms. *Biol Bull* 194: 44–52.
 52. Place SP, Smith BW (2012) Effects of Seawater Acidification on Cell Cycle Control Mechanisms in *Strongylocentrotus purpuratus* Embryos. *PLoS ONE* 7: e34068. 10.1371/journal.pone.0034068.
 53. Takeuchi K, Yokosawa H, Hoshi M (1979) Purification and characterization of hatching enzyme of *Strongylocentrotus intermedius*. *European J Biochem* 100: 257–265. 10.1111/j.1432-1033.1979.tb02056.x.
 54. Roe JL, Lennarz WJ (1990) Biosynthesis and secretion of the hatching enzyme during sea urchin embryogenesis. *J Biol Chem* 265: 8704–8711.
 55. Sweet H, Amemiya S, Ransick A, Minokawa T, McClay DR, et al. (2004) Blastomere isolation and transplantation. In: Ettensohn CA, Wessel GM, Wray GA, editors. *Method Cell Biol* 74. Amsterdam, The Netherlands: Elsevier Academic Press. 244–272.
 56. Hörstadius S (1939) The mechanics of sea urchin development, studied by operative methods. *Biol Rev* 14: 132–179. 10.1111/j.1469-185X.1939.tb00929.x.
 57. Armstrong AF, Blackburn HN, Allen JD (2012) A novel report of hatching plasticity in the phylum Echinodermata. *Amer Nat*. In press.
 58. Wolpert L (1992) Gastrulation and the evolution of development. *Development* 116: 7–13.
 59. Anderson D, Hedgecock D (2010) Inbreeding depression and growth heterosis in larvae of the purple sea urchin *Strongylocentrotus purpuratus* (Stimpson). *J Exp Mar Biol Ecol* 384: 68–75. 10.1016/j.jembe.2009.12.005.
 60. Williams GC (1975) *Sex and Evolution*. Princeton, NJ: Princeton University Press. 200 p.
 61. Hammond LM (2010) Physiological response to environmental variation in *Strongylocentrotus purpuratus* early developmental stages. Santa Barbara, CA: University of California, Santa Barbara. 195 p.
 62. Peled-Kamar M, Hamilton P, Wilt FH (2002) Spicule Matrix Protein LSM34 Is Essential for Biomineralization of the Sea Urchin Spicule. *Exp Cell Res* 272: 56–61. 10.1006/excr.2001.5398.
 63. Adomako-Ankomah A, Ettensohn CA (2011) P58-A and P58-B: Novel proteins that mediate skeletogenesis in the sea urchin embryo. *Dev Biol* 353: 81–93. 10.1016/j.ydbio.2011.02.021.
 64. Catarino A, De Ridder C, Gonzalez M, Gallardo P, Dubois P (2012) Sea urchin *Arbacia dufresnei* (Blainville 1825) larvae response to ocean acidification. *Polar Biol* 35: 455–461. 10.1007/s00300-011-1074-2.
 65. Yu PC, Matson PG, Martz TR, Hofmann GE (2011) The ocean acidification seascape and its relationship to the performance of calcifying marine invertebrates: Laboratory experiments on the development of urchin larvae framed by environmentally-relevant pCO₂/pH. *J Exp Mar Biol Ecol* 400: 288–295. 10.1016/J.Jembe.2011.02.016.
 66. McClintock JB, Amsler MO, Angus RA, Challenger RC, Schram JB, et al. (2011) The Mg-Calcite Composition of Antarctic Echinoderms: Important Implications for Predicting the Impacts of Ocean Acidification. *J Geol* 119: 457–466. 10.1086/660890.
 67. Shilling FM (1995) Morphological and physiological responses of echinoderm larvae to nutritive signals. *Am Zool* 35: 399–414.
 68. Reitzel AM, Webb J, Arellano S (2004) Growth, development and condition of *Dendaster excentricus* (Eschscholtz) larvae reared on natural and laboratory diets. *J Plankton Res* 26: 901–908.
 69. Fenaux L, Strathmann MF, Strathmann RR (1994) Five tests of food-limited growth of larvae in coastal waters by comparisons of rates of development and form of echinoplutei. *Limnol Oceanogr* 39: 84–98.
 70. Miner BG (2007) Larval feeding structure plasticity during pre-feeding stages of echinoids: Not all species respond to the same cues. *J Exp Mar Biol Ecol* 343: 158–165. 10.1016/j.jembe.2006.11.001.
 71. Adams DK, Sewell MA, Angerer RC, Angerer LM (2011) Rapid adaptation to food availability by a dopamine-mediated morphogenetic response. *Nature Comm* 2: 592. 10.1038/ncomms1603.
 72. Stumpp M, Wren J, Melzner F, Thorndyke MC, Dupont ST (2011) CO₂ induced seawater acidification impacts sea urchin larval development I: Elevated metabolic rates decrease scope for growth and induce developmental delay. *Comp Biochem Phys A* 160: 331–340. 10.1016/J.Cbpa.2011.06.022.
 73. Martin S, Richier S, Pedrotti ML, Dupont S, Castejon C, et al. (2011) Early development and molecular plasticity in the Mediterranean sea urchin *Paracentrotus lividus* exposed to CO₂-driven acidification. *J Exp Biol* 214: 1357–1368. 10.1242/jeb.051169.
 74. Miner B (2011) Mechanisms underlying feeding-structure plasticity in echinoderm larvae. In: Flatt T, Heyland A, editors. *Mechanisms of Life History Evolution: the genetics and physiology of life-history traits and trade-offs*. Oxford, England: Oxford University Press. 221–229.
 75. O'Donnell MJ, Todgham AE, Sewell MA, Hammond LM, Ruggiero K, et al. (2010) Ocean acidification alters skeletogenesis and gene expression in larval sea urchins. *Mar Ecol Prog Ser* 398: 157–171. 10.3354/meps08346.
 76. McEdward LR (1996) Experimental Manipulation of Parental Investment in Echinoid Echinoderms. *Am Zool* 36: 169–179. 10.1093/icb/36.2.169.
 77. Shingleton AW (2011) Evolution and regulation of growth and body size. In: Flatt T, Heyland A, editors. *Mechanisms of Life History Evolution: the genetics and physiology of life-history traits and trade-offs*. Oxford, England: Oxford University Press. 43–55.
 78. Pörtner HO, Dupont S, Melzner F, Storch D, Thorndyke MC (2010) Studies of metabolic rate and other characters across life stages. In: Riebesell U, Fabry VJ, Hansson L, Gattuso J-P, editors. *Guide to best practices for ocean acidification research and data reporting*. Luxembourg City, Luxembourg: Publications Office of the European Union.
 79. Lamare M, Barker M, Byrne M, Uthicke S, McCarthy A, et al. (2010) Reducing seawater pH to levels predicted for 2100 depresses larval metabolism by approximately one-third. 9th International Larval Biology Symposium. Wellington, New Zealand.
 80. Padilla-Gamiño J, Kelly M, Hofmann GE (2012) Effects of multiple stressors: impacts of elevated temperature and pCO₂ in the larval physiology of the purple sea urchin *Strongylocentrotus purpuratus*. 10th International Larval Biology Symposium. Berkeley, CA.
 81. Matson PG, Yu PC, Sewell MA, Hofmann GE (2012) Development under elevated pCO₂ conditions does not affect lipid utilization and protein content in early life history stages of the purple sea urchin, *Strongylocentrotus purpuratus*. *Biol Bull*. In press.
 82. Hammond LM, Hofmann GE (2012) Early developmental gene regulation in *Strongylocentrotus purpuratus* embryos in response to elevated CO₂ seawater conditions. *J Exp Biol* 215: 2445–2454. 10.1242/jeb.058008.
 83. Stumpp M, Dupont S, Thorndyke MC, Melzner F (2011) CO₂ induced seawater acidification impacts sea urchin larval development II: Gene expression patterns

- in pluteus larvae. *Comp Biochem Phys A* 160: 320–330. 10.1016/J.Cbpa.2011.06.023.
84. Hart MW, Strathmann RR (1994) Functional Consequences of Phenotypic Plasticity in Echinoid Larvae. *Biol Bull* 186: 291–299.
85. Cohen AL, Holcombe M (2009) Why Corals Care About Ocean Acidification: Uncovering the Mechanism. *Oceanography* 22: 118–127. 10.5670/oceanog.2009.102.
86. Pearse JS, McClintock JB, Bosch I (1991) Reproduction of Antarctic benthic marine-invertebrates - tempos, modes, and timing. *Am Zool* 31: 65–80.
87. Morgan SG (1995) Life and death in the plankton: Larval mortality and adaptation. In: McEdward LR, editor. *Ecology of Marine Invertebrate Larvae*. Boca Raton, FL: CRC Press LLC. 279–321.
88. Rumrill SS (1990) Natural mortality of marine invertebrate larvae. *Ophelia* 32: 163–198.
89. Brey T, Pearse JS, Basch LV, McClintock JB, Slattery M (1995) Growth and production of *Sterechinus neumayeri* (Echinoidea: Echinodermata) in McMurdo Sound, Antarctica. *Mar Biol* 124: 279–292.